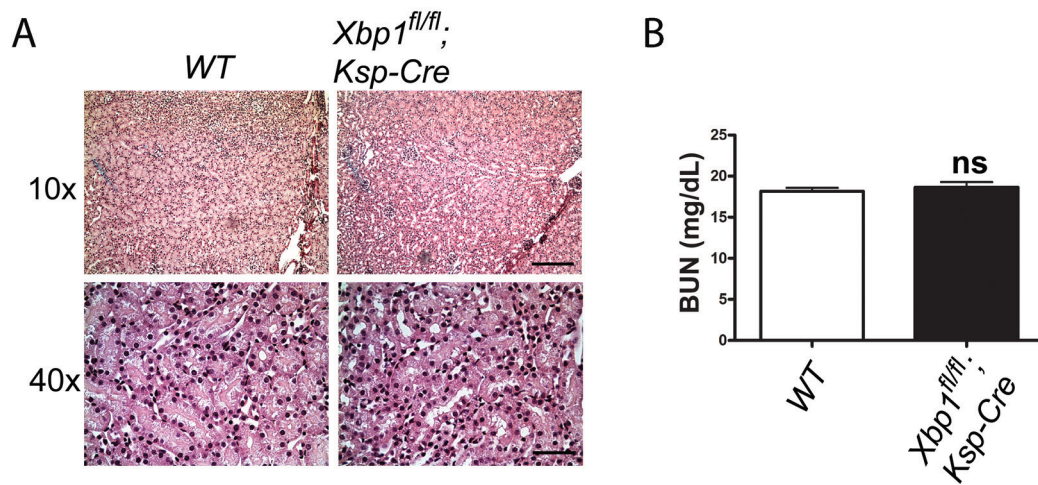
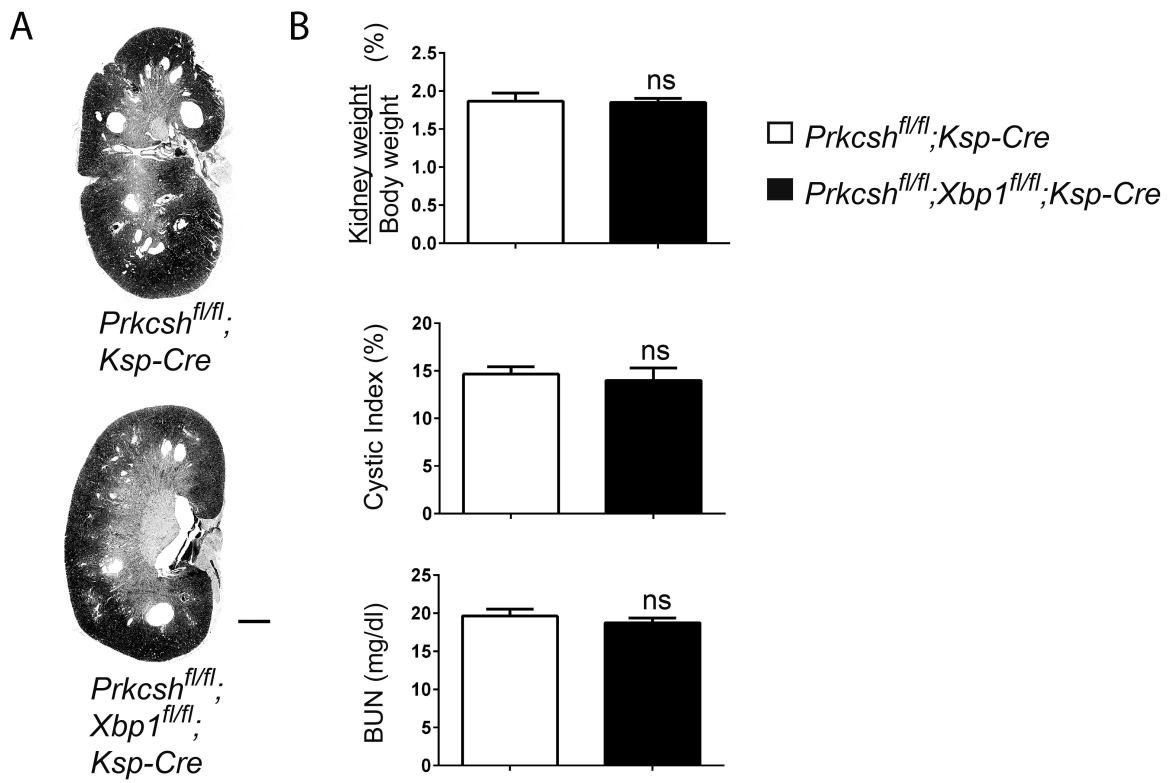


**Figure S1. Kidney sections stained with hematoxylin and eosin.** Images for all of the individual sections used in Figure 2C. Scale bar, 1 mm.



**Figure S2. Deletion of *Xbp1* using *Ksp-Cre* does not cause any morphological or functional defects in the kidney.** (A) Kidney sections from WT (*Xbp1<sup>fl/fl</sup>*) and XBP1 deficient (*Xbp1<sup>fl/fl</sup>;Ksp-Cre*) mice at 6 months of age were stained with hematoxylin and eosin. Scale bars, 500  $\mu$ m (10x); 100  $\mu$ m (40x). (B) Kidney function was assessed by BUN assay.  $n=3-4$ ;  $P=0.65$  (ns, not significant).



**Figure S3. Effects of concomitant inactivation of *Xbp1* and *Prkcsh* on cyst formation. (A)** Representative kidney sections from *Prkcsh*-only and *Prkcsh/Xbp1*-double knockout kidneys at P42 showing no change in cyst severity. **(B)** Aggregate data showing no differences in kidney weight to body weight ratio, cystic index or BUN levels;  $n = 3-4$ .

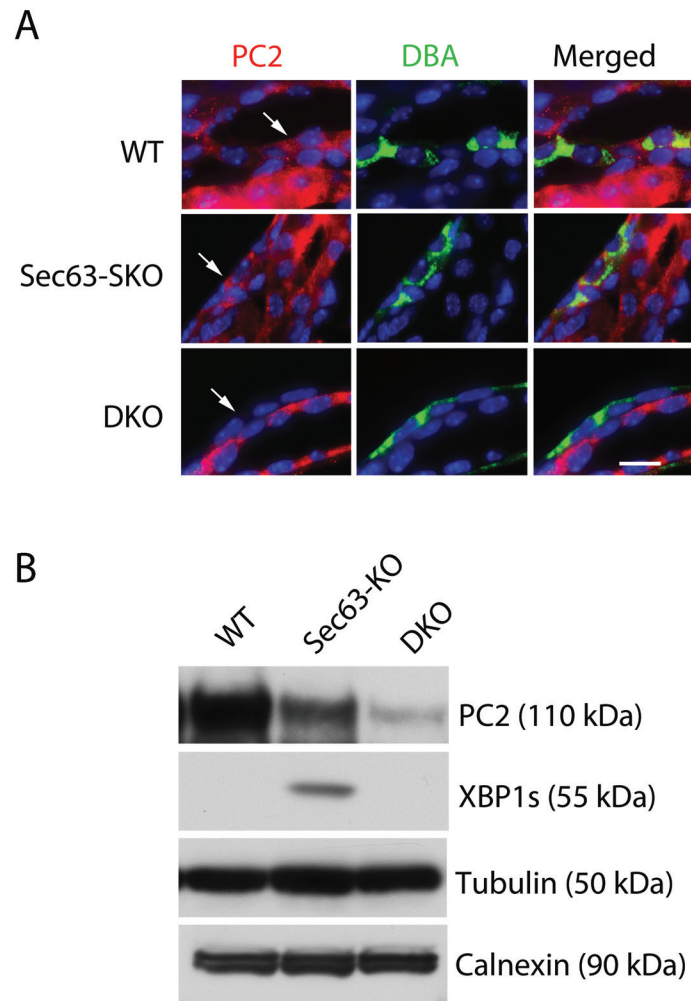


**Figure S4. Steady state PC2 levels are further decreased in DKO mouse kidneys. (A)** PC2 expression in collecting duct cyst lining cells (arrows) is progressively reduced in Sec63-KO and DKO tissues, respectively. PC2 detection by immunofluorescent staining using an anti-native PC2 antibody (YCC2). Scale bar, 5  $\mu$ m. **(B)** Progressive reduction of PC2 expression in the kidney tissue by genotype. Whole kidney lysates were subjected to immunoblotting analysis with anti-PC2 and anti-XBP1s antibodies. Tubulin and calnexin serve as loading controls.

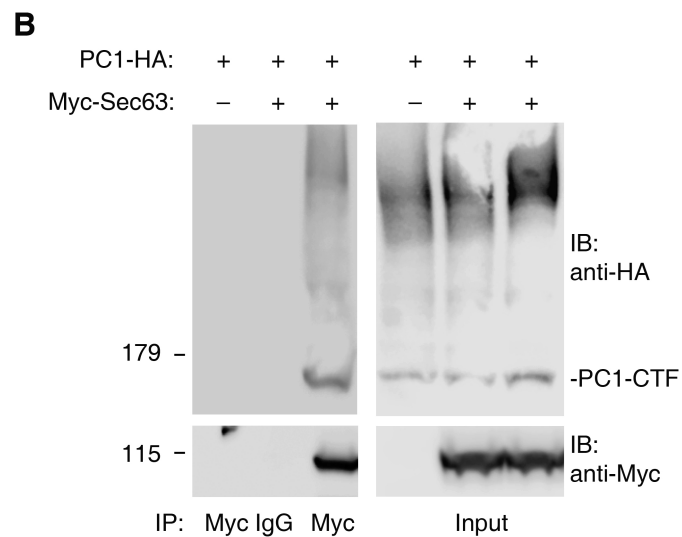
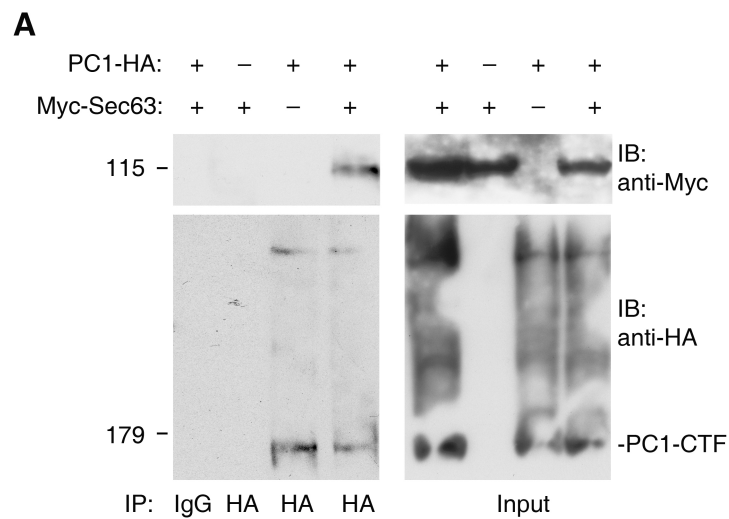


**Figure S5. Interaction between Sec63 and polycystin-1. (A)** HEK293T cells were co-transfected with PC1-HA and Myc-Sec63 plasmids as indicated. PC1 protein was immunoprecipitated (IP) using anti-HA antibody. PC1 and Sec63 proteins in immunoprecipitates and lysates were detected by immunoblotting (IB) with anti-HA and anti-Myc antibodies, respectively. **(B)** Immunoblotting was performed as indicated following immunoprecipitation of Sec63 using anti-Myc antibody.

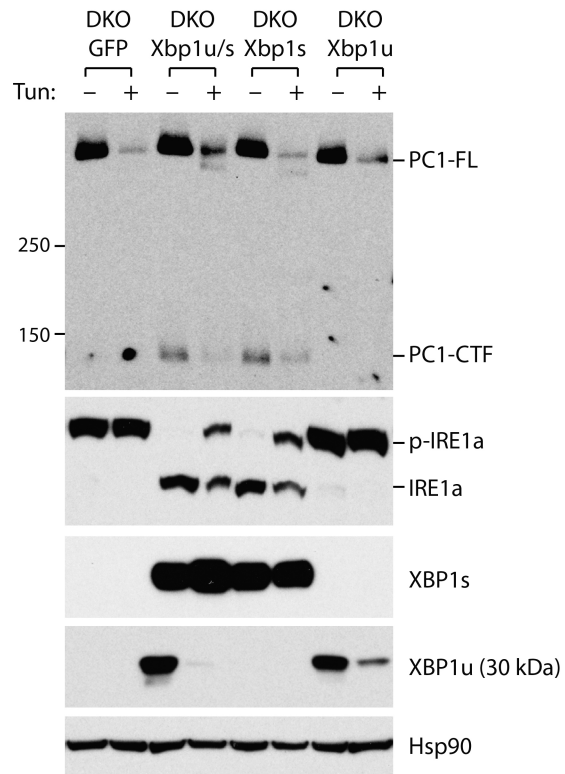


**Figure S6. PC1-CTF cleavage is induced in DKO-*Pkd1<sup>F/H</sup>*-BAC cells by XBP1s, but not by the mutant XBP1u that cannot be spliced by IRE1 $\alpha$ .** DKO-*Pkd1<sup>F/H</sup>*-BAC cells were retrovirally transduced with mouse XBP1u/s, XBP1u, and XBP1s. Cells were either unstressed or treated with tunicamycin (1  $\mu$ g/ml) for 6h, and subjected to immunoblotting analysis with indicated antibodies.

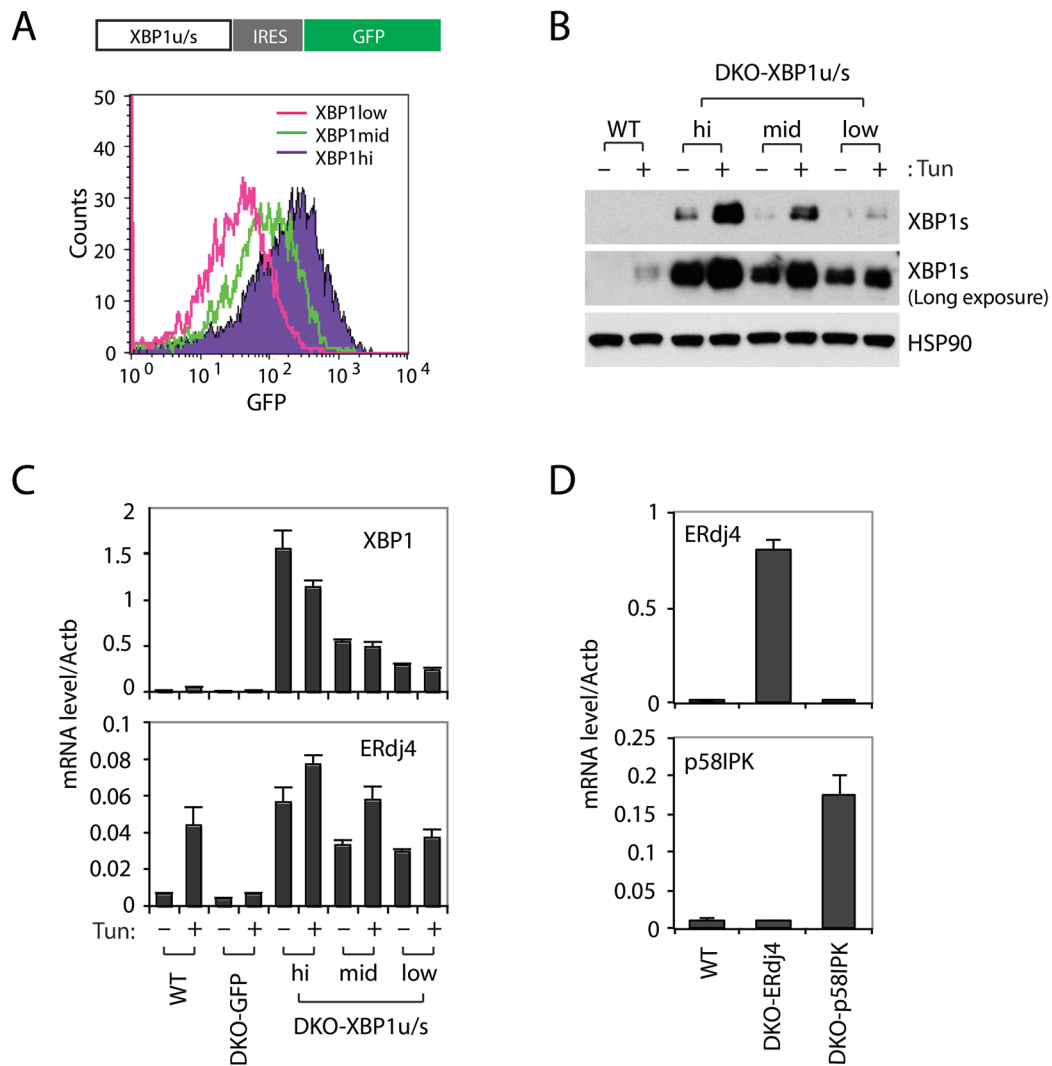


**Figure S7. Effects of XBP1 and its target genes on PC1 autoproteolytic cleavage in DKO-*Pkd1*<sup>F/H</sup>-BAC cells.** (A) The retroviral constructs possess IRES-GFP as a marker. DKO-*Pkd1*<sup>F/H</sup>-BAC cells were infected with XBP1s retrovirus at varying doses. GFP levels were determined by FACS analysis. (B) XBP1s protein levels were determined by immunoblotting in cell lines, each expressing a different level of XBP1s. (C) XBP1 and ERdj4 mRNA levels were determined by quantitative RT-PCR. (D) DKO-*Pkd1*<sup>F/H</sup>-BAC cells were infected with ERdj4 or p58IPK retroviruses. The transgene expression was examined by quantitative RT-PCR.



**Figure S8. Kidney sections stained with hematoxylin and eosin.** Images for all of the individual sections used in Figure 6E. Scale bar, 1 mm.

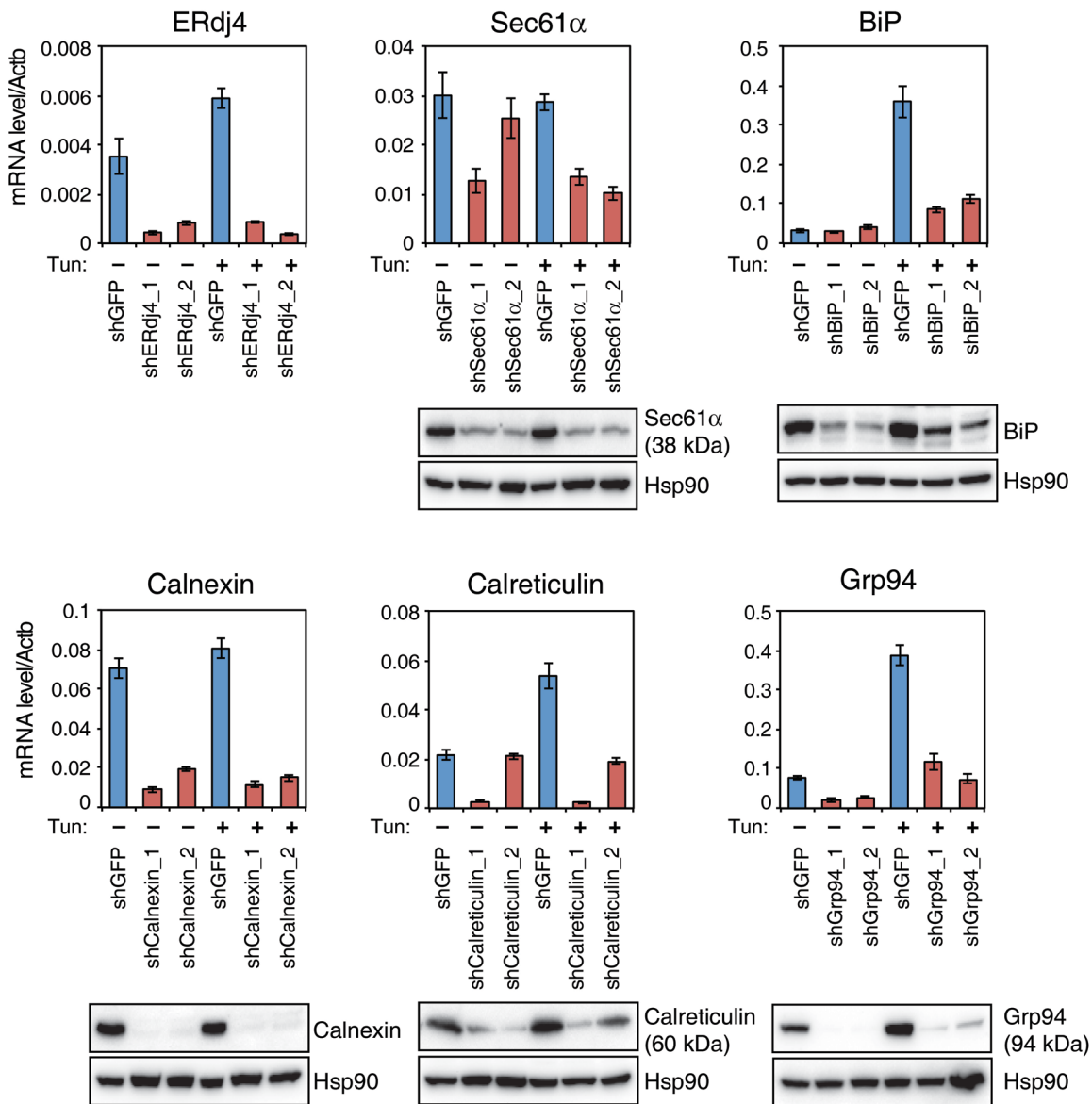


**Figure S9. Assessment of ER chaperone knockdown efficiency.** Total RNA and protein were extracted from DKO-*Pkd1<sup>FH</sup>*-BAC cells transduced with shRNA lentiviruses. Quantitative RT-PCR and western blotting were performed.

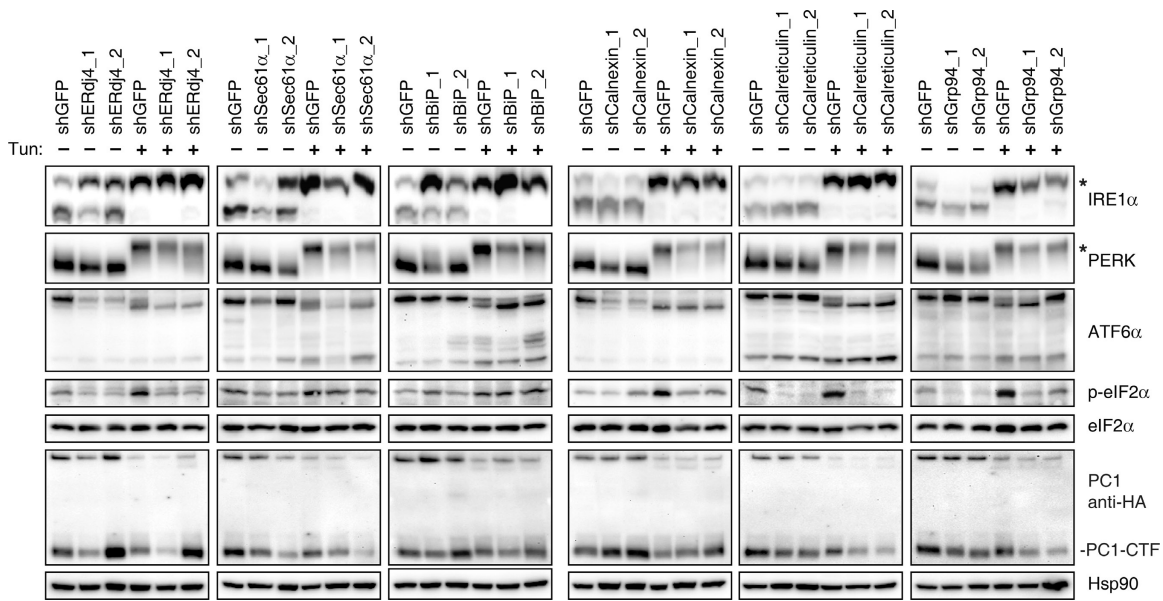


**Figure S10. Effects of chaperone silencing on IRE1 $\alpha$  activity and PC1 processing in Xbp1 deficient cells.** XBP1 deficient  $\Delta Xbp1$ -*Pkd1*<sup>F/H</sup>-BAC cells were transduced with lentiviruses expressing two independent shRNAs labeled “1” and “2” targeting the indicated genes, without and with tunicamycin. Activation status of UPR sensors and PC1 processing were determined by immunoblotting. \*, active phosphorylated form of the respective UPR sensors.

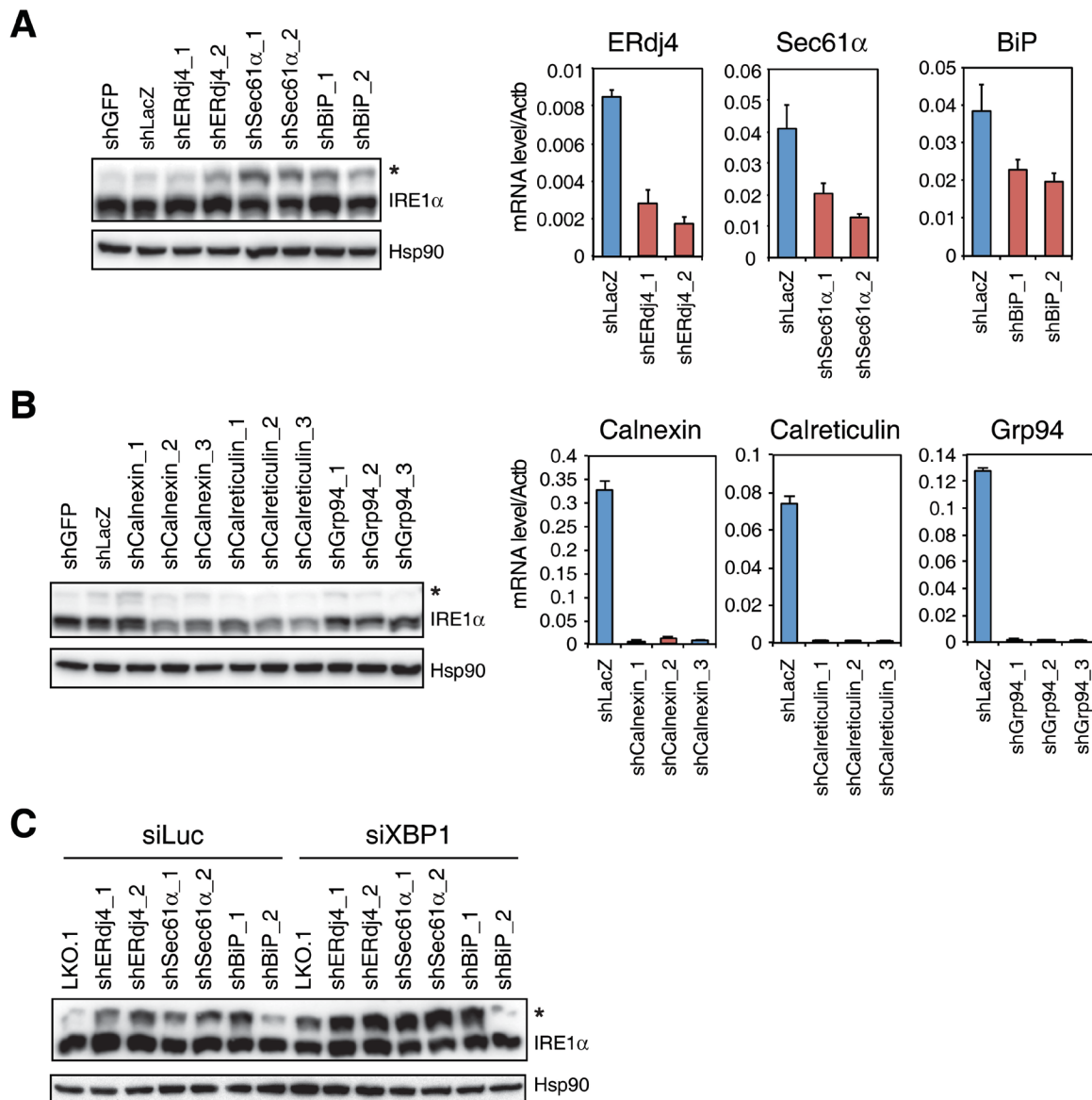


**Figure S11. IRE1 $\alpha$  activity in Hepa1-6 cells expressing shRNAs targeting ER chaperones. (A)** Hepa1-6 cells were transduced with lentiviruses expressing shRNAs targeting ERdj4, Sec61 $\alpha$  or BiP. IRE1 $\alpha$  phosphorylation was assessed by PhosTag western blotting. Knockdown efficiency was measured by quantitative RT-PCR. GFP and LacZ targeting shRNAs were used as controls. **(B)** Effects of calnexin, calreticulin and Grp94 shRNAs on IRE1 $\alpha$  activity. **(C)** shRNA-transduced Hepa1-6 cells were transiently transfected with luciferase or XBP1 siRNA. IRE1 $\alpha$  phosphorylation was assessed by PhosTag western blotting.